Permafrost Distribution in Central Canada: Applications of a Climate-Based Predictive Model

Author(s): Frederick E. Nelson

Source: *Annals of the Association of American Geographers*, Vol. 76, No. 4 (Dec., 1986), pp. 550-569
Published by: Taylor & Francis, Ltd. on behalf of the Association of American Geographers
Stable URL: http://www.jstor.org/stable/2562710
Accessed: 01-04-2016 15:52 UTC

Permafrost Distribution in Central Canada: Applications of a Climate-Based Predictive Model

Frederick E. Nelson

Department of Geography, Rutgers University, New Brunswick, NJ 08903

Abstract. A revised permafrost index, computed from mean monthly air temperatures and snow-cover data, produces an unambiguous latitudinal zonation of contemporary permafrost. Isarithmic mapping of this "surface frost number" defines a latitudinal zonation that is in substantial agreement with a previous semi-empirical mapping of permafrost in the lowlands of central Canada. A related index, the "Stefan frost number," employs estimates of soil properties in an approximate engineering solution for the depths of freezing and thawing. Mapping of this index by unclassed choropleth methods provides an estimate of point-to-point variations in permafrost distribution under the assumptions of homogeneous topography and vegetation. The model successfully predicts the presence of permafrost in peatlands outside the zonal limits defined by climatic criteria alone. The frost number provides an easily computed, physically based method for predicting permafrost that lends itself to a variety of cartographic representations of permafrost distribution.

Key Words: permafrost distribution, permafrost forecasting, permafrost mapping, permafrost zonation, snow cover, soil freezing, Canada.

INVESTIGATORS concerned with the distribution of permafrost in North America usually employ a classification in which permafrost is characterized on the basis of its areal continuity. The cartographic expression of this classification is a quasi-latitudinal zonation that, proceeding from lower to higher latitudes, consists of a permafrost-free zone, a discontinuous zone in which permafrost occurs under local conditions favorable to its existence, and a continuous zone in which permafrost is present everywhere beneath the land surface. Despite frequent reference to this classification in the literature, permafrost zones have rarely been delimited using criteria that can be related unambiguously to the continuity of permafrost.

Numerous problems confront the researcher seeking to regionalize permafrost continuity on the basis of observational data. Although geophysical surveys and boreholes are the most reliable sources of information about permafrost, they are extremely costly and are possible only when the potential for economic return is large. At present, such data are available primarily from relatively small areas such as oilfields and transportation corridors. Compounding this problem, subsurface data are often proprietary and are generally unavailable.

Outside the areas of intense development, direct permafrost investigations are restricted by inadequate funding. Remote sensing and airphoto interpretation are not always viable alternatives, because of forest cover or a lack of suitable geomorphic or vegetative indicators. For example, in the discontinuous permafrost zone, palsas are regarded by some authorities (e.g., R. J. E. Brown 1974) as the only reliable surficial indication of the presence of permafrost. Palsa distribution, however, is heavily dependent on the distribution of peatlands, which are not present in many areas.

As a result of such difficulties, numerous investigators have attempted to predict permafrost distribution by means of environmental data such as averages computed from weather records. Most such attempts, however, treat only one or two of the relevant environmental parameters. An ideal method of permafrost prediction and regionalization would not only consider the effects of macroclimate but would also include such "secondary factors" as snow cover, soil thermal properties, substrate hetero-

Annals of the Association of American Geographers, 76(4), 1986, pp. 550–569

geneity, vegetation, and topoclimate. Although scale dependencies may preclude detailed cartographic depiction of the effects of such secondary variables, their influence may be apparent in a general way, even on maps depicting entire continents.

The "frost number" proposed by Nelson and Outcalt (1983) synthesizes several important variables into easily computed and readily interpreted maps of permafrost distribution. The 1983 paper presented only an outline of the method's application and emphasized estimation of freezing and thawing indices for locations with sparse or incomplete climatological data. The degree-day estimation technique used by Nelson and Outcalt (1983) yields inaccurate results for many locations; the present paper uses a procedure that is more general and is better suited to areas where monthly mean climatological data are available. The utility of this "frost number" for predicting permafrost is tested using climate data from central Canada, a region where the areal extent of permafrost is fairly well known and in which complications induced by topography are small.

The Frost Number

Permafrost indices based on the ratio of frost and thaw depths were proposed independently by Lunardini (1981, 551) and by Nelson and Outcalt (1983). The principle behind these indices is that permafrost can be expected at locations where the depth of winter freezing exceeds that of summer thaw or where the accumulation of freezing degree days is greater than that of thawing degree days. Such an index can be computed for most locations from the mean annual air temperature $\overline{T}$, the mean air temperatures ($\overline{T}_h$, $\overline{T}_c$) of the warmest and coolest months, the annual air temperature amplitude A, and precipitation data. Soil thermal properties and moisture content can also be incorporated into the calculations. The "air frost number" F, redefined here as

$$F = \frac{DDF^{1/2}}{DDF^{1/2} + DDT^{1/2}} \tag{1}$$

gives a crude prediction of the presence or absence of contemporary permafrost[1] at the location as a function of its air freezing (DDF) and thawing (DDT) indices. Equation (1) restricts the frost number to the interval [0,1], which ameliorates problems arising from underestimation of the freezing and thawing indices (Nelson and Outcalt 1983, 910–11), and allows expression of the frost number for any location. Numerical values of the index are given an interpretation in the next section.

Nelson and Outcalt (1983) obtained estimates of the freezing and thawing indices (°C days) by representing a station's temperature record as a simple cosine function and integrating this curve above and below the 0°C axis. The procedure is outlined in the following series of equations, in which temperatures are assumed to be expressed in °C:

$$A = (\overline{T}_h - \overline{T}_c)/2 \tag{2.1}$$

$$\beta = \cos^{-1}(-\overline{T}/A) \tag{2.2}$$

$$\overline{T}_s = \overline{T} + A\,\beta^{-1}\int_0^{\beta}\cos\theta\,d\theta$$

$$= \overline{T} + A(\sin\beta/\beta) \tag{2.3}$$

$$\overline{T}_w = \overline{T} + A(\pi - \beta)^{-1}\int_{\beta}^{\pi}\cos\theta\,d\theta$$

$$= \overline{T} - A[\sin\beta/(\pi - \beta)] \tag{2.4}$$

$$L_s = 365(\beta/\pi) \tag{2.5}$$

$$L_w = 365 - L_s \tag{2.6}$$

$$DDT = \overline{T}_s L_s \tag{2.7}$$

$$DDF = \overline{T}_w L_w. \tag{2.8}$$

The "frost angle" β refers to values of the radian equivalent of time, θ, at which the cosine curve crosses 0°C. Because the curve is symmetric about $\theta = \pi$, the integrations in (2.3) and (2.4) can be performed over only half the annual cycle. L_s and L_w refer to the length of summer and winter in days, respectively, and $\overline{T}_s$ and $\overline{T}_w$ represent the mean temperatures during those seasons.

Although snow cover can be the critical factor determining the presence or absence of permafrost (e.g., Granberg 1973), it is not often incorporated into studies of permafrost distribution based on climate normals (e.g., Harris 1981; Pihlainen 1962). The computations in Equation (2) can be modified to incorporate the influence of snow cover. An "average" snow depth $\overline{Z}_s$ for the winter is estimated from

$$\overline{Z}_s = \sin^2\phi\left\{\sum_{i=1}^{k} Z_{si}\,[k - (i - 1)]\right\}/k \tag{3}$$

where Z_{si} is recorded snowfall in those months i ($i = 1,2, \ldots ,k$) in which the mean temperature is 0°C or below. Reduction of the snowpack during winter resulting from periods of thaw or sublimation is assumed to be a simple trigonometric function of the station's latitude ϕ; at progressively higher latitudes a greater proportion of the snowpack remains throughout the winter.[2]

Given an average snow-cover thickness $\overline{Z}_s$, the temperature amplitude at the ground surface in winter A_+ is calculated as

$$A_+ = A \exp\{-\overline{Z}_s[\pi/(\alpha_s P)]^{1/2}\} \quad (4)$$

where P is the period of the temperature cycle and α_s is the thermal diffusivity of the snow cover, computed using the Van Dusen (Paterson 1981, 186), Dorsey (Langham 1981, 275), and Bilello (1969) formulas for thermal conductivity, specific heat capacity, and density, respectively. The subscript + indicates incorporation of the effects of snow cover in all subsequent calculations. From Equation (2.4), the mean winter surface temperature $\overline{T}_{w+}$ is

$$\overline{T}_{w+} = \overline{T} - A_+[\sin \beta/(\pi - \beta)] \quad (5)$$

and the freezing index, adjusted for snow-cover effects is

$$DDF_+ = -\overline{T}_{w+} \times L_w. \quad (6)$$

Although Equations (4)–(6) ignore nonconductive heat-transfer processes occurring in the snowpack, the approximate nature of these equations is consistent with the coarseness of the input data.[3] The final result is the "surface frost number," F_+, given by

$$F_+ = \frac{DDF_+^{1/2}}{DDF_+^{1/2} + DDT^{1/2}}. \quad (7)$$

A source of problems in the procedures outlined by Nelson and Outcalt (1983) is the assumption that a temperature curve for any location can be approximated closely by a simple cosine function computed from the extreme monthly temperatures. For many stations, incorporation of one or more additional harmonics may be required to describe the record of monthly temperatures completely (e.g., Panofsky and Brier 1968, 128–35). Cubic spline interpolation (e.g., King 1984, 166–89), however, provides a more efficient method of representing the monthly temperature series exactly and makes explicit allowance for the unequally spaced data points necessitated by use of mean monthly temperatures. The temperature curve obtained by cubic splines can be integrated numerically to obtain more accurate estimates of the freezing and thawing indices. This method of obtaining degree-day estimates requires a modification to the snow-effect computations, which is achieved by computing the mean winter air temperature $\overline{T}_w$ numerically, and using this value to solve Equation (2.4) for the quantity $\{\sin \beta/(\pi - \beta)\}$. The latter quantity is then substituted in Equation (5) to obtain $\overline{T}_{w+}$, the mean winter temperature at the surface, a procedure that, in effect, equates the observed temperature curve with a perfect sinusoid of the same amplitude and that encloses the same area below the 0°C axis.

If data on soil thermal properties and soil moisture are available or can be estimated for a region of interest, the Stefan solution or its modifications can be used to refine the frost number further. The Stefan solution (e.g., Jumikis 1977, Chs. 14 and 15) provides an estimate of the depth of frost $\overline{Z}_f$ (m) in a given soil from

$$Z_f = \left[\frac{2 \lambda_f S DDF}{\rho_d w_f L}\right]^{1/2} \quad (8)$$

where λ_f is the thermal conductivity ($W\ m^{-1}\ °C^{-1}$) of the freezing soil, ρ_d is the dry density of the soil ($kg\ m^{-3}$), w_f is the freezing soil's water content expressed as a proportion of the soil's dry weight, S is the scale factor 86,400 ($s\ day^{-1}$), and L is the latent heat of fusion ($333.66 \times 10^3\ J\ kg^{-1}$). By replacing the quantities λ_f, w_f, and DDF with the corresponding unfrozen values λ_u, w_u, and DDT, the depth of thaw Z_t can be computed for the same soil. The Stefan solution can also be extended easily for use with layered soil systems (e.g., Jumikis 1977, 209–24). By using DDF_+ to obtain an estimate of the depth of freezing in one of the Stefan solutions, a "Stefan frost number" F_{s+} incorporating snow-cover effects can be calculated as

$$F_{s+} = \frac{Z_{f+}}{Z_{f+} + Z_t}. \quad (9)$$

Equation (9) is conceptually consistent with the manner in which permafrost forms. If a permafrost-free area is suddenly exposed to subzero mean annual surface temperatures as a result of

climate change or emergence of the area from beneath a body of deep water, the depth of freezing in the first winter will exceed the depth of thaw the following summer, resulting in formation of a layer of permafrost (Lachenbruch 1968, 833). In subsequent years the permafrost will grow thicker until an equilibrium is achieved between the surface temperature and heat flow from the earth's interior. Because 30-year means are used to calculate the climatic parameters making up the frost number, Equation (9) should be regarded as a conceptual device. In areas of seasonal frost, the depth of thaw in summer obviously cannot exceed the depth to which a substrate was frozen the previous winter. Similarly, the depth of winter freezing in permafrost regions cannot exceed the thickness of the unfrozen layer existing above the permafrost table during the previous summer. Although the unmodified Stefan solution (Equation (8)) yields overestimates of the depths of both frost and thaw because it neglects the soil's heat capacity, those errors tend to cancel when the ratio is formed in Equation (9).

Interpretation and Mapping

Although the concepts of continuous, discontinuous, and sporadic permafrost are apparent intuitively, operational definitions have proven difficult to implement. Some problems involved in these definitions were reviewed by Ives (1974).

In their most basic forms, the terms *continuous, discontinuous,* and *sporadic* permafrost zones refer, respectively, to regions in which permafrost underlies all terrain units, regions where extensive areas underlain by permafrost are separated by smaller areas of seasonally frozen ground, and regions where permafrost occurrences are of small areal extent and are separated by larger areas of terrain without permafrost. In Canada, the latter zone has been called the "southernmost fringe of discontinuous permafrost" (R. J. E. Brown 1967). In a subsequent publication, Brown (1978) presented a revised terminology, in which the discontinuous zone was divided into subzones with "widespread" or "scattered" permafrost. However, the definitions of these subzones are identical to those of the "discontinuous" and "sporadic" zones in the older terminology, which will be retained in this paper.

In the sporadic zone, occurrences of permafrost are (1) attributable to topoclimatic effects, (2) a consequence of localized ground cover or soil properties, or (3) relics from past colder climatic intervals and not in thermal equilibrium with the present climate. Without paleoclimatic estimates, the frost number is incapable of predicting the location of relict permafrost. Because of the small geographical scale and relatively level terrain in the study area delimited below, only continuous and discontinuous permafrost zones will be discussed in the remainder of this paper.

Surface Frost Number

The surface frost number F_+ is used to establish a latitudinal zonation of permafrost at small geographical scales, with zones defined as follows: (1) no permafrost: $0 \leq F_+ < 0.5$; (2) discontinuous permafrost: $0.5 \leq F_+ < 0.66\overline{6}$; and (3) continuous permafrost: $F_+ \geq 0.66\overline{6}$. The interpretation assigned to Case (1) is based on the fact that $F_+ < 0.5$ reflects a thawing index, DDT, larger than the corresponding surface freezing index, DDF_+. An isoline connecting points where $F_+ = 0.5$ therefore defines the boundary of "climatic permafrost" (Heginbottom 1984), i.e., permafrost predicted solely on the basis of climatic criteria. This boundary also represents the 0°C isotherm at the ground surface, providing a physical justification for its placement. It may, however, provide an underestimate of the extent of contemporary permafrost because the thermal properties of some soils (e.g., peat under certain hydrologic conditions) are such that the calculated depth of frost penetration can exceed that of thaw despite equal freezing and thawing indices at the surface.

Case (2) defines the discontinuous permafrost zone, in which permafrost may exist given favorable soil thermal properties and ground cover. Nelson and Outcalt (1983) based their upper limit of this subdivision ($F_+ = 0.60$ using Equation (7)) on visual correlations of isoline position with Péwé's (1975) boundary in Alaska and that of R. J. E. Brown (1967) in northwestern Canada. Portions of Péwé's and Brown's continuous/discontinuous permafrost boundaries, however, were drawn on the basis of cri-

teria that cannot easily be related to the continuity of permafrost, suggesting that the isoline used by Nelson and Outcalt (1983) may be a poor choice for a zonal permafrost boundary.

Although the "continuous permafrost zone" represented by Case (3) is a simple geographical concept, operational definitions advanced in the literature involve numerous qualifications as well as aspatial criteria. Some workers have argued that the equatorward limit of continuous permafrost coincides with a line joining sites at which the temperature at the level of zero annual amplitude is −5°C (e.g., Brown and Péwé 1973, 75). Such data are not readily available, however, necessitating use of an assumed constant relationship between this temperature and mean annual air temperature (e.g., R. J. E. Brown 1967). There is little basis for the latter assumption because spatial variations in snow cover, soil moisture, and soil thermal properties, as well as vegetation and topoclimatic effects, lead to wide variations in air-ground temperature differences (e.g., Lunardini 1981, 144–46).

Representation of the continuous/discontinuous boundary by the value −5°C at the level of zero annual amplitude is a long-standing practice inherited from early Soviet investigations and can be traced through Muller (1945) to Sumgin (1940). Apparently, the basis for this criterion is the assumption that a temperature of −5°C at this level at an arbitrary location is sufficiently cold that all nearby terrain units will also be underlain by permafrost, regardless of soil properties, ground cover, or other factors. It is, therefore, a rather oblique method for delineating regions in which permafrost is spatially continuous.

A more justifiable procedure for defining regions of continuous permafrost makes use of W. G. Brown's (1964) observation that for any given freezing index, the depth of frost penetration will vary by no more than a factor of two for the range of (mineral) soils and moisture contents found in nature. A similar relationship can be expected to hold for thawing soils (Brown 1964, 225). These relationships suggest that at locations where $DDF_+/DDT = 4.0$, that is, where Equation (7) yields $F_+ = \frac{2}{3}$, the smallest Stefan frost number obtainable is $F_{s+} = 0.5$, so that permafrost can be expected to be continuous around such locations. Because the thermal properties of any particular soil will not vary so radically between the frozen and unfrozen states, this boundary is conservative in that it may underestimate the areal extent of continuous permafrost in regions of predominantly level terrain and homogeneous ground cover.

Stefan Frost Number

Because the Stefan frost number F_{s+} employs information about the substrate, its application is not restricted to simple climate-based latitudinal zonations. The increased spatial resolution obtained by incorporating soils data allows treatment of point-to-point variations in permafrost conditions, although the assumptions of level terrain and uniform vegetative cover are maintained in this paper.

Two types of map can be constructed using the Stefan frost number. In the first, soil properties are considered to be uniform over the map area, and the distribution of permafrost is examined as a function of climate for that soil type. A series of isarithmic maps, each map representing a different soil type, provides an indication of whether permafrost can be expected at selected locations, for any specified combination of soil characteristics.

A second type of map can be constructed by using a grid to sample soil types over the area of interest. By estimating soil thermal properties for each soil type, a value of F_{s+} can be computed for each grid cell using Equation (9) or its equivalent for layered soil sytems. Because boundaries between soil types are sharp, the information on such maps is best presented in a raster or choropleth format, rather than by isarithmic mapping.

Unless the thickness of snow cover is highly variable, the concept of discontinuous permafrost is not relevant in the first type of mapping. In general, permafrost can be expected poleward of the 0.5 F_{s+} isoline in any occurrence of the specified soil. Conversely, discontinuous permafrost can be central to the second type of mapping and is easily communicated through an appropriate cartographic strategy. Continuity of permafrost on such maps is determined by the contiguity of cells in which $F_{s+} \geqslant 0.5$. "Continuity" is therefore a rather subjective determination and is highly dependent on map scale, cell size, and the extent to which the assumptions of terrain and vegetative homogeneity are satisfied. Some possibilities for mapping F_{s+} are explored in the next section.

Permafrost Distribution in Central Canada

Climate and Physiography

To test the utility of the frost number, an area of central Canada was selected for a series of computations (Fig. 1a). The area is bounded roughly by the 70th and 49th parallels on the north and south, respectively, on the east by an arc connecting the U.S.-Manitoba-Ontario border, Churchill Manitoba, and the northwest tip of the Melville Peninsula, and on the west by an arc joining the U.S.-Alberta border near the Rocky Mountain front, High Level Alberta, and Darnley Bay in the Amundsen Gulf. The region includes Saskatchewan, Manitoba, and most of Alberta, as well as parts of the Districts of Mackenzie, Keewatin, and Franklin. With the exception of small areas of hills and mountains in the northwest, the terrain has low relief (Bostock 1970). Because climate-permafrost relationships are less complex in this region than elsewhere in North America (Brown and Péwé 1973, 75), it was selected for a test of the frost-number methodology. The land surface within

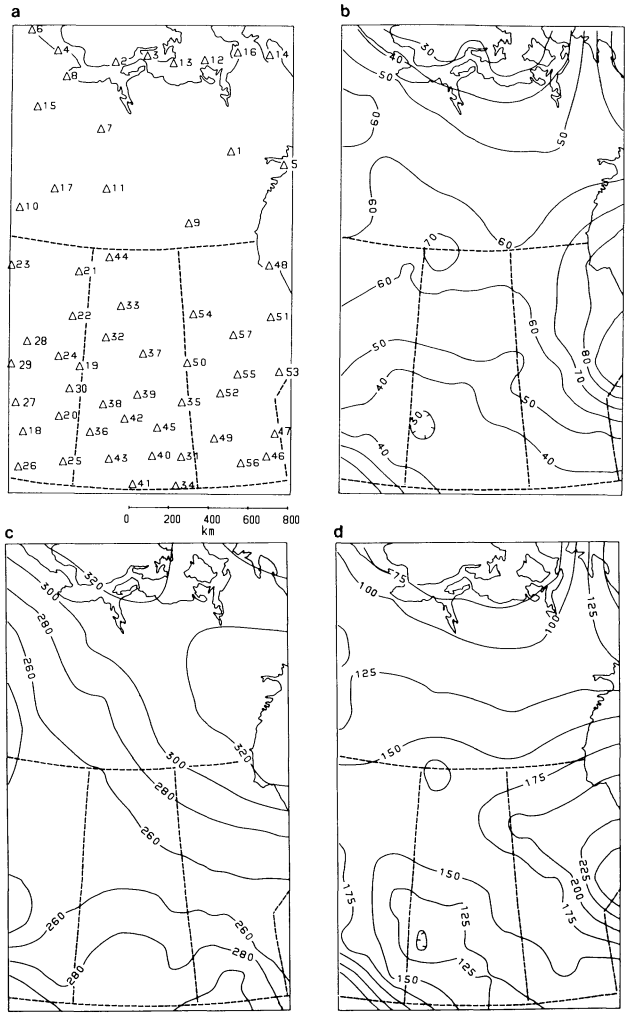

Figure 1. (a) Station locations; stations are identified in Table 1. (b) "Average" snow-cover thickness $\overline{Z}_s$ (cm). (c) Estimated snow density ρ_s (kg m^{-3}). (d) Annual snowfall $\sum_{i=1}^{k} Z_{si}$ (cm).

Table 1. Key to Station Codes Shown in Figure 1a

Northwest Territories	Saskatchewan
1 Baker Lake	31 Broadview
2 Byron Bay	32 Buffalo Narrows
3 Cambridge Bay A	33 Cree Lake
4 Cape Young	34 Estevan A
5 Chesterfield	35 Hudson Bay
6 Clinton Point	36 Kindersley
7 Contwoyto Lake	37 La Ronge A
8 Coppermine	38 North Battleford A
9 Ennadai Lake	39 Prince Albert A
10 Fort Providence	40 Regina A
11 Fort Reliance	41 Rockglen
12 Gladman Point A	42 Saskatoon A
13 Jenny Lind Island A	43 Swift Current A
14 Pelly Bay	44 Uranium City A
15 Port Radium	45 Wynyard
16 Shepherd Bay A	Manitoba
17 Yellowknife	46 Beausejour
Alberta	47 Bissett
18 Calgary International A	48 Churchill A
19 Cold Lake A	49 Dauphin A
20 Coronation A	50 Flin Flon
21 Fort Chipewyan A	51 Gillam A
22 Fort MacMurray A	52 Grand Rapids
23 High Level A	53 Island Lake
24 Lac la Biche A	54 Lynn Lake
25 Medicine Hat A	55 Norway House
26 Pincher Creek Town	56 Portage la Prairie A
27 Rocky Mountain House	57 Thompson A
28 Slave Lake	
29 Whitecourt	
30 Vermilion	

the map area can be regarded at this scale as an inclined plane, sloping gently from approximately 1,000 m above sea level in the southwest to sea level in the north and east.

A standardized set of 30-year (1951–1980) mean monthly climate data was used for all computations (Canada Atmospheric Environment Service 1982a;b;c;d); station locations are shown in Figure 1a. With one exception (Chesterfield), only stations shown on the map, *Principal Climatological Station Network* (Canada Atmospheric Environment Service 1982e), were employed. Although 75 such stations lie in the area shown in Figure 1a, they are concentrated south of 55°N, a situation that could have adverse effects in the statistical applications described below. This problem was addressed by determining the map distance between the two stations closest to one another north of 55°N and using this distance as a criterion for eliminating stations south of 55°N. Groups of stations closer than the specified distance (135 km) were delimited, and stations within each group were assigned arbitrary integers. Pseudo-random numbers were then generated and used to eliminate stations until no two closer than the specified distance remained. If a group consisted of only two stations, a coin toss was employed to delete one. This procedure is advantageous because it always leads to a more uniform areal coverage than the original distribution but cannot result in total elimination of points in any subarea of the map.

The resulting distribution of 57 points, used for all subsequent analyses, is shown in Figure 1a. The nearest neighbor index (Clark and Evans 1954) yields a value of 1.48, indicating a tendency toward a uniform rather than clustered distribution. All subsequent isarithmic maps were constructed by creating a 34 × 21 grid from the original 57 points using a "lattice-tuning" interpolation technique (Tobler 1979).

Most of the study area is subject to a continental climatic regime with large annual temperature ranges and light precipitation. Mean annual air temperatures and Conrad's (1946) index of continentality are shown in Figures 2a and 2b, respectively; the smooth temperature pattern reflects the region's subdued topographic relief. Despite the relatively high elevation of the southwest, isotherms form a strong northwest-southeast alignment over the entire map area, reflecting a decrease of mean annual temperature from southwest to northeast. This arrangement is a consequence for the severity and duration of winter, during which a similar pattern evolves as a result of the trajectory of arctic air incursions (Hare and Thomas 1979, 103), supplemented by the effects of chinook winds in the southwest. During summer, the highest mean temperatures are found in the southeast, although strong temperature gradients are not present in the southern half of the map area.

The map of "average snow-cover thickness" (Figure 1b), computed using Equation (3), is similar in form to that of annual snowfall (Figure 1d). Values rise from the north and south map borders to an east-west oriented zone of high values in the central portion of the map. The highest values occur in east-central Manitoba, centered on Island Lake. This station is located on the lee shore of a large water body and experiences heavy snowfall early in winter, before the lake is frozen over. A similar situation exists at Uranium City, Saskatchewan on Lake Athabasca. The map of estimated snow density (Figure 1c) depicts increasing density from southwest to northeast, a reflection of the influence of both temperature and wind speed in Bilello's (1969) equation.

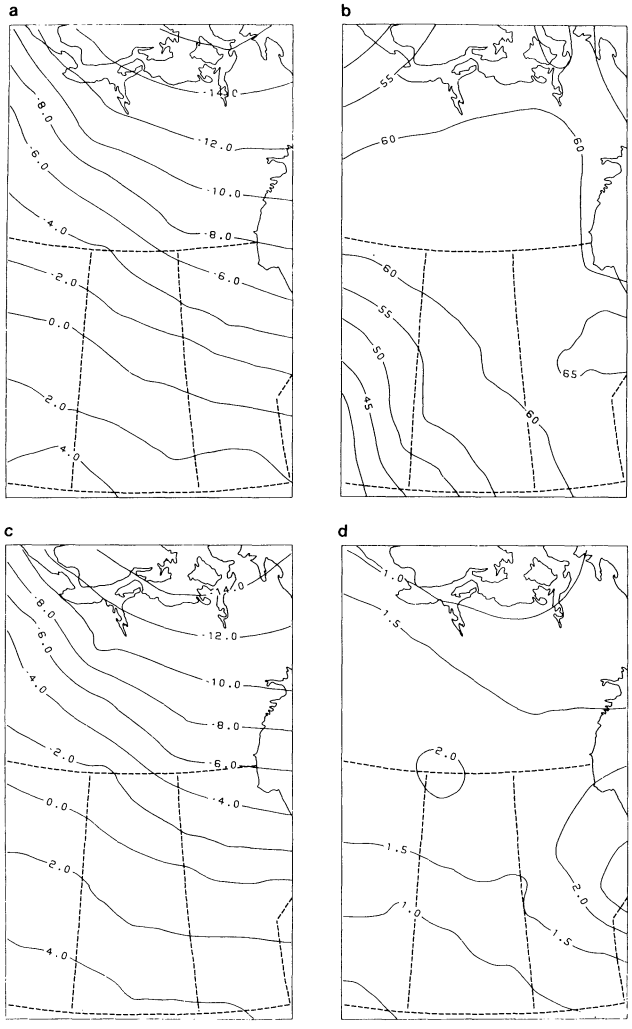

Figure 2. (a) Mean annual air temperature $\overline{T}$ (°C). (b) Conrad's continentality index; potential values range from zero (ultra-oceanic) to 100 (ultra-continental). (c) Mean annual surface temperature $\overline{T}_+$. (d) Difference map obtained in subtracting $\overline{T}$ matrix from $\overline{T}_+$ matrix.

Figure 2c shows mean annual temperatures adjusted for snow-cover effects; individual isotherms are displaced northward by 150–200 km relative to their positions in Figure 2a. The pattern of isotherms in this map is virtually identical to that in Figure 2a, except for the northward curvature of two isolines in east-central Manitoba caused by the thick snow cover in this vicinity. Figure 2d is a difference map obtained by subtracting the matrix of air temperatures (Fig. 2a) from that of surface temperatures (Fig. 2c); the map depicts a surface similar in form to that of snow cover (Figure 1b). Again, the largest values (2–3°C) occur at Island Lake, Manitoba and Uranium City, Saskatchewan.

Maps of the screen-level thawing and freezing indices (Figs. 3a and 3b, respectively) are similar in form to those of the mean summer and winter air temperature fields (not shown). The pattern of discrepancies between the *DDF* (Fig. 3b) and DDF_+ (Fig. 3c) maps is, of course, similar to that between the $\overline{T}$ and $\overline{T}_+$ maps (Figs. 2a and 2c). The magnitudes of these differences (Fig. 3d) range from under 300 (Jenny Lind Island) to nearly 1,000 (Island Lake) freezing degree days, or from 3 percent (Jenny Lind Island) to 53 percent (Pincher Creek) of those

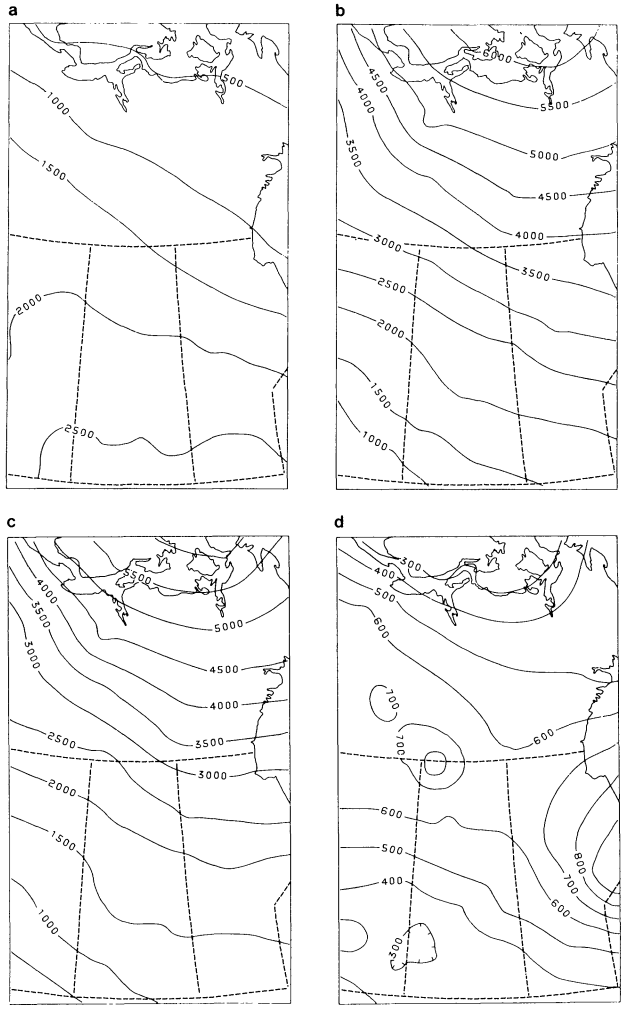

Figure 3. (a) Air thawing index *DDT* (°C days). (b) Air freezing index *DDF*. (c) Surface freezing index DDF_+. (d) Difference map obtained by subtracting DDF_+ matrix from *DDF* matrix; surface represents reduction of freezing index attributable to presence of snow cover.

available climatologically. Figures 2d and 3d illustrate the importance of incorporating snow cover in any climate-based permafrost forecasting technique.

Surface Frost Number

The air and surface frost numbers defined by Equations (1) and (7) are mapped isarithmically in Figures 4a and 4b. R. J. E. Brown's (1967) permafrost boundaries are also included on these maps. In this area of Canada, Brown's boundaries were based on a combination of field observation and assumed air-ground temperature relationships. Although Brown's southern limit of permafrost coincides roughly with the −1°C (30°F) mean annual air isotherm, Zoltai (1971) has shown that permafrost occurs in peatlands considerably south of this isotherm. Brown's (1967) boundary between the discontinuous and continuous permafrost zones was placed along the −8.3°C (17°F) isotherm "to correspond with a mean annual ground temperature of 23°F" (−5°C), except for a southward flexure on the west side of Hudson Bay, where his field observations indicated a narrow zone of continuous permafrost. However, the continuity of permafrost in the latter area has been questioned recently (French and Gilbert 1982).

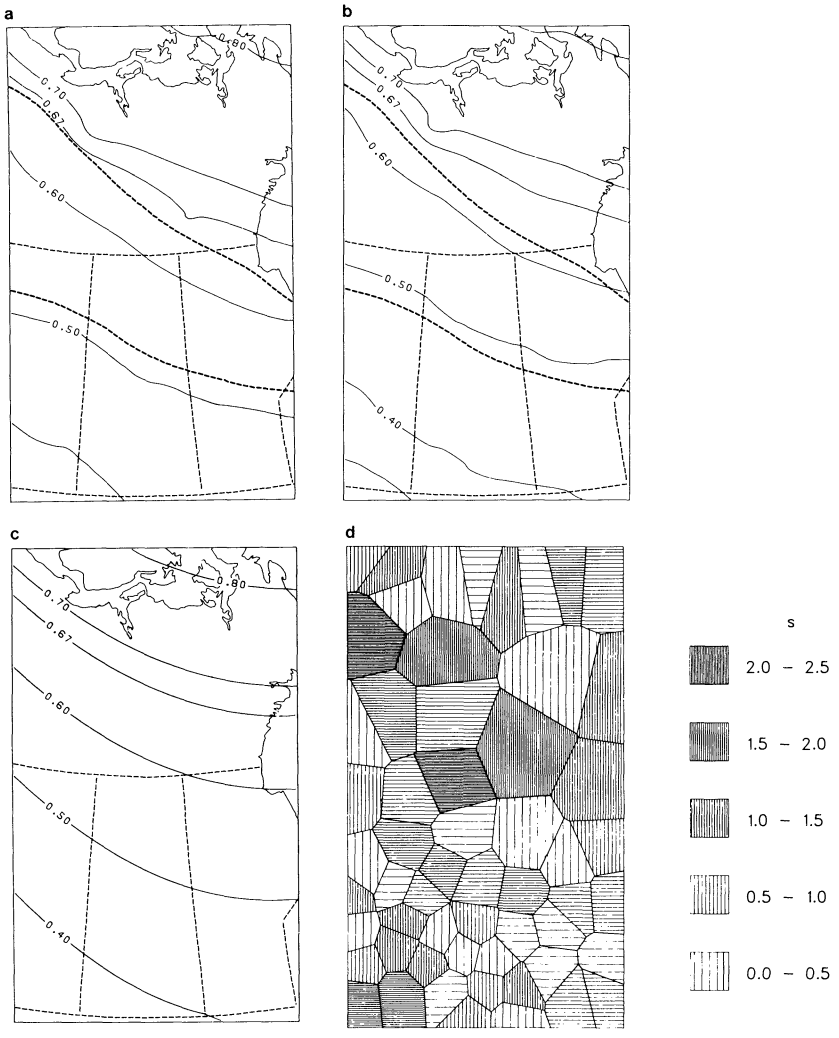

Figure 4. (a) Air frost number F. (b) Surface frost number F_+. Southern limit of discontinuous permafrost is represented by 0.5 isoline; limit of continuous permafrost corresponds to 0.67 isoline. Heavy dashed lines in (a) and (b) are R. J. E. Brown's (1967) zonal permafrost boundaries. (c) Map of surface frost number constructed from quadratic trend surface (Eq. (10)). (d) Residuals from quadratic trend surface, displayed in Thiessen diagram generated from 57 sample points shown in Figure 1a. Thiessen network forms basis for binary adjacency matrix used in tests for spatial autocorrelation. Residuals are distributed as N(0,1) after standardization. Intervals are in units of standard deviation (s = 0.0185) from the actual mean value (0.000). Positive and negative residuals are represented by vertical and horizontal shading, respectively.

Perhaps the most striking feature of Figures 4a and 4b is the similarity of each with the maps of mean annual air and surface temperatures, respectively (Figs. 2a and 2c). In the absence of a pronounced continentality gradient, mapping the frost number produces a surface similar to the corresponding mean temperature field. Superposition of the air and surface frost-number maps reveals, however, localized divergence of the isolines in areas where snow cover is heavy, as well as a more general parallel displacement. In the west-central part of the map area, where snow cover is thick and relatively uniform, the 0.5 and 0.6 surface (F_+) frost-number isolines are displaced approximately 200 km relative to those on the air (F) frost-number map. In east-central Manitoba, where snow cover is thickest, however, this offset is supplemented by northward curvature of the 0.5 isoline. This pattern illustrates not only the

importance of considering snow cover in mapping permafrost boundaries, but also the capability of the frost number to cut across mean annual air isotherms. Because the 0.5 isoline on Figure 4a is identical with the 0°C mean annual air isotherm, it falls about 100 km south of R. J. E. Brown's (1967) boundary for the southern limit of permafrost. The effects of snow cover are such that the corresponding isoline in Figure 4b falls approximately 100 km north of Brown's southern limit.

Isarithmic maps such as Figure 4b provide only a generalized summary of the underlying data array. The smooth surface represented by the map of F_+ suggests the possibility that zonal permafrost boundaries in central Canada could be accurately represented by a relatively simple mathematical function. This assertion was examined by computing trend surfaces of orders 1 through 3 for the F_+ data (Table 2). The extremely high goodness of fit for all three equations affirms that the boundaries can be represented well by a simple equation. Selection of the most appropriate model was made by (1) visual correlation of the isoline pattern produced by the trend-surface equations with the map of F_+, (2) evaluation of the spatial autocorrelation among residuals from the trend surfaces, and (3) statistical testing to assess the significance of added terms. All three procedures indicated that the quadratic equation produced adequate results, and only the quadratic trend surface and its residuals are illustrated (Figs. 4c and 4d).

Visual assessment of the correspondence between maps was made by superimposing each trend-surface map on Figure 4b. This is the most subjective of the three procedures but indicates that the quadratic and cubic equations yield good summaries of isoline position. Both are large improvements over the linear equation, which cannot produce curvature. Because there was no discernible improvement in the map yielded by the cubic equation over that produced by the quadratic, the latter was deemed better on the basis of the simplicity of its generating equation.

Table 2. Goodness of Fit (R^2) for Trend Surfaces[a]

Surface	Goodness of fit
Linear	0.973
Quadratic	0.981
Cubic	0.982

[a] All surfaces are statistically significant at $p \leq 0.01$.

Residuals from the three trend surfaces were tested for spatial autocorrelation using the procedure outlined by Cliff and Ord (1981, 198–203) under assumption N (normality). Two weighting matrices were employed: (1) a binary adjacency matrix based on the Thiessen diagram (Rhynsburger 1973) shown in Figure 4d and (2) a weight assignment computed as the inverse of the map distances between pairs of points. Both weighting matrices are symmetric; elements of the binary matrix were given the value unity if the corresponding polygons shared an edge. Because the linear equation is incapable of producing isoline curvature, clusters of both positive and negative residuals exist, and the null hypothesis of no spatial autocorrelation was rejected for both types of weighting schemes. In contrast, the null hypothesis was retained for residuals from the quadratic and cubic trend surfaces for both sets of weights. In the interest of simplicity the quadratic surface was again selected as the better model. In all cases, the inverse-distance weighting scheme yields lower values of the test statistic I.

Tests for the significance of adding higher-order terms (Davis 1973, 342–43) led to the same conclusions as procedures (1) and (2). This series of tests indicated that introduction of quadratic terms yields a statistically significant improvement over the linear surface, while the cubic surface is not an improvement over the quadratic.

These results demonstrate that permafrost boundaries can be accurately represented by simple mathematical functions in areas of low relief. For the study area, the equation

$$F_+ = 0.299 + 0.160 \times 10^{-3}X_1 + 0.148 \times 10^{-3}X_2 - 0.637 \times 10^{-7}X_1^2 + 0.885 \times 10^{-8}X_1X_2 + 0.123 \times 10^{-7}X_2^2 \quad (10)$$

in which X_1 and X_2 are eastings and northings (km) from an arbitrary origin at the southwest map corner, accounts for 98.1 percent of the variation in the data set.

Stefan Frost Number

Computed over an areal unit, the surface frost number distills several input variables (freezing index, thawing index, snow thickness) and

yields a smooth field that (1) provides a physically justified latitudinal zonation of contemporary permafrost, (2) is easily interpreted, and (3) is represented accurately by a simple mathematical expression. However, the surface frost number estimates only the configuration of the classical (latitudinal) permafrost zonation. Greater spatial resolution requires incorporation of subsurface information and involves computations with the Stefan frost number, which requires mapping strategies other than those considered above.

Uniform Soil Properties. To demonstrate use of the Stefan frost number F_{s+} and "uniform" soil properties, four maps with increasing soil-profile complexity were prepared (Fig. 5). Frost and thaw depths were computed for each element of the 34 × 21 DDT and DDF_+ grids using Equation (8) or its equivalent for layered soil systems. The soil properties used in these computations are given in Table 3.

As noted earlier, the surface frost number F_+ may yield an underestimate of the equatorward limit of permafrost. Because soil thermal conductivity is often higher in the frozen than in the unfrozen state, incorporation of soil properties in the frost number may cause an equatorward displacement of the permafrost "boundary" relative to its position as given by F_+. These displacements are shown as shaded areas in Figure 5.

Soil 1. This simple example (Fig. 5a) uses a single-layer silt-clay soil with mid-range values of dry density, water content, and thermal conductivity (Harlan and Nixon 1978, 116). Because of the presence of an appreciable pore fraction occupied by water, the ratio λ_f/λ_u of the thermal conductivities in the frozen and unfrozen states is 1.2. This is reflected by an equatorward displacement of the permafrost boundary and other isolines relative to a mapping of F_+ (Fig. 4b), placing it close to R. J. E. Brown's (1967) permafrost limit. North of the boundary $F_{s+} = 0.5$, permafrost can be expected for any soil with these thermal properties, although permafrost-free areas could be anticipated at locations with extremely thick snow cover.

Soil 2. The multilayer Stefan solution was used to obtain values of F_{s+} for a two-layer soil system comprised of a layer identical to the preceding example, capped by an organic layer 5 cm thick. Superposition of Figure 5b on Figure 5a suggests that addition of the organic layer results in a relatively small (<100 km) equatorward displacement of the permafrost boundary. At higher latitudes, however, southward displacement of isolines is considerable (>250 km), whereas south of the permafrost boundary they are displaced northward slightly. At locations with large DDF_+/DDT ratios, the depth of thaw, already small in Soil 1, is reduced further by the insulating properties of the organic layer, increasing the value of F_{s+} and causing a large equatorward displacement of the isolines in the northern part of the map area. Near the permafrost boundary, however, where the freezing and thawing indices are nearly equal, displacement of the isolines is a function primarily of the ratio of thermal conductivity between the frozen and unfrozen states. Stated alternatively, removal of the organic layer in higher latitudes results in only a moderate percentage increase in the depth of freezing but a large percentage increase in the depth of thaw. Conversely, near the permafrost boundary, the percentage changes in frost or thaw penetration depths induced by addition or removal of an organic layer are similar in magnitude, and displacement of the F_{s+} isolines is relatively small.

Soil 3. A three-layer soil system with properties similar to those of the Nekik Lake Soil of west-central Manitoba (Tarnocai 1972) was used to predict the distribution of permafrost in a soil/terrain unit in which palsas and other peat-related permafrost landforms are common. The basal layer is a silt-clay soil identical to Soil 1. The middle layer consists of one meter of peat with a water content of 200 percent (percent dry weight), overlain by 50 cm of peat with the same dry density but a water content of 120 percent.

The permafrost boundary for Soil 3 (Fig. 5c) lies 200–400 km south of its position on previous maps, in substantial agreement with Zoltai's (1971, 308) "southern limit of permafrost features in peatland" in Manitoba and Saskatchewan and considerably south of R. J. E. Brown's (1967) "southern limit of permafrost." This result suggests that the shaded area of Figure 5c could be used to define a zone of "sporadic" permafrost.

Estimated frost and thaw depths in Soil 3 are much smaller than in Soil 1, owing to the peat's large volumetric latent heat and relatively low thermal conductivity (e.g., Paré 1984). The pattern of isoline displacement relative to Soil 1 is the opposite of that produced by Soil 2; a large southward displacement of the permafrost

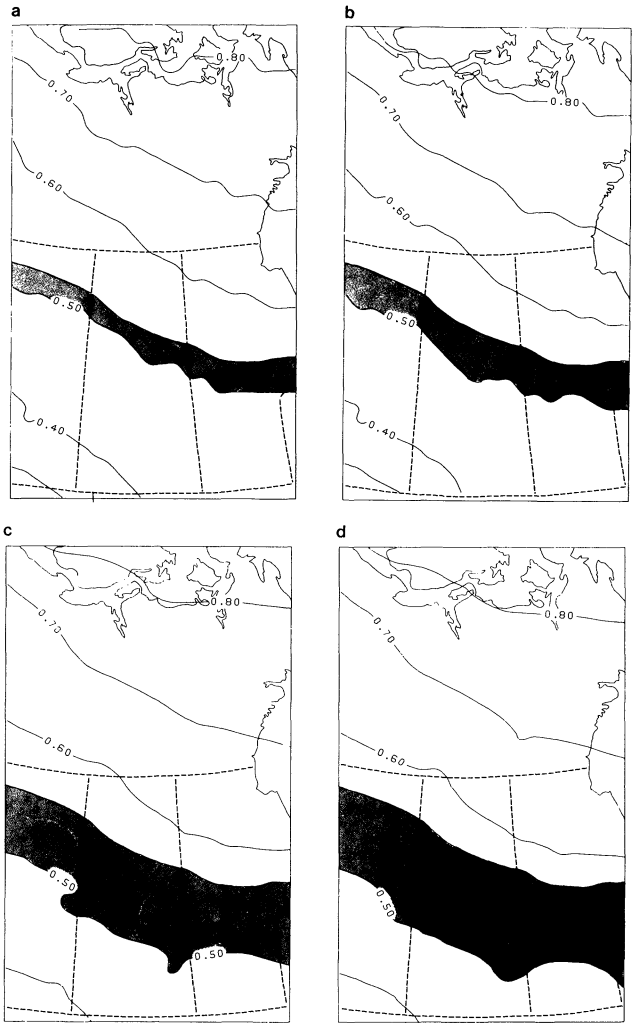

Figure 5. Stefan frost number, computed for uniform soil properties. Soil thermal properties used in computations are listed in Table 3. Shaded areas represent southward displacement of permafrost boundary (0.50 isoline) relative to that of surface frost number shown in Figure 4b. (a) Soil 1; (b) Soil 2; (c) Soil 3; (d) Soil 4.

border ($F_{s+} = 0.5$) is apparent, but isoline dislocations are smaller in the northern part of the map.

The divergence of the southern boundary of permafrost for Soil 3 relative to that for Soil 1 results from unequal reductions of the depths of frost and thaw. In the southern part of the map area, the two peat layers result in absolute reductions in the depths of thaw that are much greater than those for the depths of freezing. Because the thermal conductivities of the peat layers are much lower in the unfrozen state, the frost number is most affected at locations in the southern portions of the map, where thawing indices are largest. The exception to this general pattern occurs in the northeastern portion of the map, the only area where freezing indices are large enough to allow penetration of frost into all three soil layers. At such locations (e.g., Gladman Point, Pelly Bay) the large increment of freezing depth in the relatively high thermal conductivity, low water-content silt-clay layer causes a relatively large southward displacement of the 0.8 isoline.

Soil 4. Soil 4 is identical to Soil 3 in all respects except that the uppermost 5 cm dries during summer, as may be expected in the higher portions of peatlands. This soil system

Table 3. Soil Properties Used for Input to Stefan Solution, Uniform Soils (see Fig. 5)

	λ_f	λ_u	w_f	w_u	ρ_d	Z_i
Soil 1	1.20	1.00	0.20	0.20	1400	semi-infinite
Soil 2						
Layer 1	0.20	0.14	0.80	0.80	300	0.05
Layer 2	1.20	1.00	0.20	0.20	1400	semi-infinite
Soil 3						
Layer 1	0.35	0.22	1.20	1.20	300	0.50
Layer 2	0.75	0.40	2.00	2.00	300	1.00
Layer 3	1.20	1.00	0.20	0.20	1400	semi-infinite
Soil 4						
Layer 1	0.35	0.14	1.20	0.80	300	0.05
Layer 2	0.35	0.22	1.20	1.20	300	0.45
Layer 3	0.75	0.40	2.00	2.00	300	1.00
Layer 4	1.20	1.00	0.20	0.20	1400	semi-infinite

results in a relatively uniform southward displacement of the isolines by approximately 40–50 km (Fig. 5d) relative to their position represented on the map for Soil 3. The interpretation for this case is straightforward; thaw depths are slightly smaller than those in Soil 3, resulting in a slight increase in the frost number at all stations. Although the modification of F_{s+} values is somewhat larger at high-latitude stations, the changes in Z_t are very small and do not translate into large displacements of F_{s+} isoline positions as they would if the layer of variable moisture content were thicker.

Nonuniform Soil Properties. A map of F_{s+} using spatially variable soil properties was prepared by sampling broad soil classes in the study area from the map *Soils of Canada* (Canada Department of Energy, Mines and Resources 1972), using a 34 × 21 grid. Coarse approximations of soil properties were made by using descriptions of representative profiles in Clayton et al. (1977) to establish values for soils with similar textural and moisture properties from Harlan and Nixon's (1978, 115–17) nomograms of Kersten's (1949) data. Dry density for soils in broad textural classes was obtained from Jumikis (1977, 64), and soil moisture content was inferred from conditions depicted on the map *Soil Climates of Canada* (Canada Department of Energy, Mines and Resources 1975). The estimated soil characteristics for the 17 soil types employed in the analysis are listed in Table 4; for simplicity, only single-layer soils were employed, with the exception of Soil 17. The upper layer of the latter soil system (a Cryic Fibrisol in the Canadian system of soil classification) occurs only in the arctic and subarctic and was restricted to a thickness of 1.5 m, in keeping with the observation that organic soils are usually thin in such regions (e.g., MacFarlane 1969, 243). Soil properties used for the lower layer in this soil system are those of the Cryic Regosol (Soil 13) common in northern Canada. The distribution of soil types in the study area is represented in Table 5.

The 34 × 21 matrices of DDT and DDF_+ (Figs. 3a and 3c) were used in conjunction with the appropriate soil properties (Tables 4 and 5) as input to a program that computes the multilayer Stefan solution for each grid cell and returns matrices of Z_t, Z_f, and F_{s+}. The program also generates graphic output to convey this information. At locations where the soils map indicated "Rockland Land Type" (<10 cm of unconsolidated surficial material), the program uses Terzaghi's (1952, 22) equation

$$Z_r = [12\ \alpha_r\ t]^{1/2} \tag{11}$$

to estimate the level Z_r (m) to which perceptible temperature changes occur in the absence of phase change. Lithology was obtained from the *Geological Map of Canada* (Geological Survey of Canada 1970) and estimates of thermal diffusivity α_r ($m^2\ s^{-1}$) for the two generalized rock types present at the surface in the study area were obtained from Johnston et al. (1981, 119). The durations t (seconds) of the freezing and thawing seasons at each station were computed in the spline interpolation routine and mapped onto regular lattices by the method used for degree-day estimates.

Because the soils map is on a nominal scale of measurement, isarithmic mapping is poorly suited for this application. Isarithmic maps

Table 4. Soil Properties Used as Input for Stefan Solution, Nonuniform Soils (see Figs. 6 and 7)

Code[a]	Canada Dept. of Energy, Mines and Resources (1972) map symbol	Soil type	λ_f	λ_u	w	ρ_d
1	A1	Brown Chernozemic	1.60	1.50	0.12	1600
2	A2	Dark Brown Chernozemic	1.60	1.50	0.12	1600
3	A3	Black Chernozemic	2.00	1.70	0.15	1600
4	A4	Dark Gray Chernozemic	1.00	0.90	0.15	1400
5	B1	Brown Solonetz	1.00	1.00	0.12	1600
6	B2	Black Solonetz	1.70	1.40	0.20	1600
7	C2	Gray Luvisol	1.25	1.20	0.15	1600
8	D3	Humo-Ferric Podsol	1.90	1.40	0.20	1400
9	E2	Eutric Brunisol	1.80	1.40	0.25	1600
10	E3	Dystric Brunisol	1.25	1.20	0.15	1600
11	F1	Orthic Regosol	1.50	1.40	0.10	1600
12	F2	Cumulic Regosol	1.25	1.00	0.20	1400
13	F3	Cryic Regosol	1.80	1.40	0.25	1600
14	G1	Humic Gleysol	1.70	1.40	0.20	1600
15	G2	Gleysol	1.90	1.40	0.20	1400
16	H1	Fibrisol	0.75	0.40	2.00	300
17	H3	Cryic Fibrisol[b]	0.75	0.40	2.00	300

[a] Numbers correspond to entries in Table 5.
[b] Values shown apply to upper 1.5 m of Soil 17; lower layer is same as Soil 13.

could display a visually disconcerting array of peaks, pits, and inflections in areas encompassing soils with dissimilar thermal properties, even under a smooth temperature field. For this application, raster or choropleth methods are superior. The F_{s+} data are ideally suited for application of Tobler's (1973) unclassed choropleth mapping technique by virtue of restriction of the range of data values to the interval [0,1]. Graytones in each cell can be made exactly proportional to data values, subject to an adjustment for perceptual response. Thus, in cells where $F_{s+} = 0.8$, the proportion of inked paper is also approximately 0.8, where $F_{s+} = 0.5$, approximately 50 percent of the cell is inked, and so on.

Figure 6 is an example of this type of document for the central Canada map area. Although the southern boundary of permafrost depicted on this map is somewhat tortuous, few "islands" of permafrost occur within generally permafrost-free areas and vice versa because the effects of terrain climate, vegetation, and other complicating factors were not included in the computations. The dominant pattern in Figure 6 reflects increasing values of F_{s+} from southwest to northeast, in response to the field of mean annual temperature. Within this general trend, minor deviations occur, as with the lighter shading associated with thick snow cover in the vicinity of Island Lake and locally darker cells associated with peatlands.

Although the unclassed choropleth approach provides a good overall impression of the F_{s+} pattern for a map area, the ratio nature of the index precludes depiction of any information about the predicted depths of frost or thaw penetration. Another type of map was devised to portray this information (Fig. 7); in this map the axes of an ellipse represent frost and thaw depths, and shading density within each ellipse is proportional to the cell's F_{s+} value, as with Figure 6. In Figure 7, the length of an ellipse's horizontal axis is proportional to the depth of potential frost penetration, while the vertical axis is proportional to the potential depth of thaw. The axes are scaled so that the representation of the maximum Z_f or Z_t value is equal to the width of the grid cells. On maps such as Figure 7, a station that experiences a large freezing index but little or no thawing would be represented by a horizontal line. Locations at which frost and thaw depths are equal are represented by circles, while one with little or no freezing would be depicted by a vertical line. Although not as pleasing aesthetically as Figure 6, the ellipse map contains a great deal more information. In Figure 7, for example, small ellipses in

Table 5. Matrix of Codes Referencing Soil Types[a]

13	0	0	13	13	13	13	13	13	13	13	13	0	0	0	13	13	0	0	0	0
13	13	13	0	0	13	13	13	13	13	13	13	0	0	13	0	13	13	13	−2	0
13	13	13	13	0	13	13	13	0	0	0	0	0	0	13	0	0	13	13	13	0
13	13	13	13	0	0	0	0	13	13	0	0	0	0	13	13	13	13	13	13	13
0	17	13	13	13	13	13	13	13	13	13	13	13	13	13	13	13	13	13	13	13
0	17	10	10	13	13	13	13	13	13	13	13	13	13	13	13	13	13	13	13	13
0	0	10	10	10	13	13	13	13	13	13	13	13	13	13	13	13	13	13	13	13
17	17	10	10	10	13	13	13	13	13	13	13	13	13	13	13	13	13	13	13	13
17	17	10	10	10	10	13	13	13	13	13	13	13	13	13	13	13	13	13	13	13
17	17	10	10	10	10	13	13	13	13	13	13	13	13	13	13	13	13	13	13	13
17	17	10	10	10	10	10	13	13	13	13	13	13	13	13	13	13	13	13	13	13
17	17	10	10	10	10	10	10	13	13	10	13	0	13	13	13	13	13	13	13	0
17	9	9	0	10	0	10	10	10	13	10	10	10	10	10	10	13	13	13	0	0
9	9	0	0	0	8	8	8	10	10	10	10	10	10	10	10	13	13	13	0	0
15	15	9	14	14	8	8	8	8	8	10	10	10	10	10	10	10	10	10	0	0
15	15	15	9	14	−1	8	8	8	8	8	8	0	10	10	10	10	10	10	0	0
15	17	17	7	15	−1	−1	8	8	8	8	8	8	8	8	8	8	10	10	0	0
15	17	17	16	16	−1	0	8	8	8	8	8	8	8	8	8	8	8	8	17	0
7	16	16	16	12	8	8	8	8	8	8	8	8	8	8	8	8	8	17	17	17
7	16	16	16	12	8	8	8	8	8	8	8	8	8	8	8	9	7	7	17	17
7	16	7	16	16	16	8	8	8	8	8	8	0	8	8	16	7	7	7	17	17
7	16	16	16	16	16	7	8	8	8	8	8	8	8	16	16	16	16	7	17	17
7	16	16	16	16	16	7	8	8	8	8	8	8	16	16	16	16	16	7	7	7
7	16	7	16	16	16	7	16	7	8	8	8	8	16	8	8	16	16	7	7	7
7	16	7	7	7	7	7	7	7	16	7	16	8	8	7	7	16	16	16	7	7
7	7	3	3	7	7	7	7	7	7	7	16	16	7	14	16	16	16	16	16	16
7	3	3	6	3	3	3	7	7	7	7	4	7	16	7	7	0	0	16	16	16
7	3	3	6	2	11	3	3	3	11	3	3	4	7	16	0	7	0	16	16	−1
7	3	3	5	2	2	2	2	2	2	3	3	7	7	4	4	7	7	0	16	−1
3	3	2	5	5	1	1	2	11	2	11	3	3	4	7	3	4	4	7	16	−1
3	2	2	5	1	1	1	1	1	2	3	3	3	3	3	7	3	3	4	4	0
3	2	1	1	1	1	1	2	1	2	2	2	3	3	3	3	3	3	3	3	3
3	3	1	1	2	2	2	1	1	1	1	5	2	3	3	3	3	3	3	3	3
0	0	0	1	1	1	1	1	1	2	2	2	2	2	3	0	0	0	0	0	0

[a] Positive code numbers correspond to soil types listed in Table 4. Negative values indicate "Rockland Land Type"; −1 and −2 indicate granite and quartzite, respectively. Zeros indicate water bodies or U.S. territory.

the southern part of the map represent thick peat deposits in which the depth of both frost and thaw penetration are small due to the relatively low thermal conductivity and large volumetric latent heat of the material. The depths of freeze and thaw in such materials are considerably less than, for example, in a silt or clay soil subject to the same surface climate. Depiction of these locations in an unmodified choropleth or isarithmic format reflects only the higher F_{s+} value resulting from the strong divergence between values of thermal conductivity of moist peat in the frozen and unfrozen states. Figure 7 combines a good visual impression of the frost number's variation with retrievable quantitative estimates of frost and thaw penetration. Proportional shading could also be used to depict other scalar fields, such as mean annual temperature or permafrost thickness.

Conclusions

The frost number is a simple, easily interpreted, and physically based forecasting tool that can be used to construct rational and well-defined zonal permafrost boundaries on small-scale maps. Application of the surface frost number to central Canada yields a latitudinal zonation of contemporary permafrost that is in substantial agreement with R. J. E. Brown's (1967) semi-empirical mapping. This distribution, expressed as an isarithmically mapped scalar field, is accurately summarized by a quadratic expression obtained by trend-surface methods.

Results from the Stefan frost number demonstrate that permafrost "boundaries" are sensitive to soil properties and suggest that the surface frost number can underestimate the areal

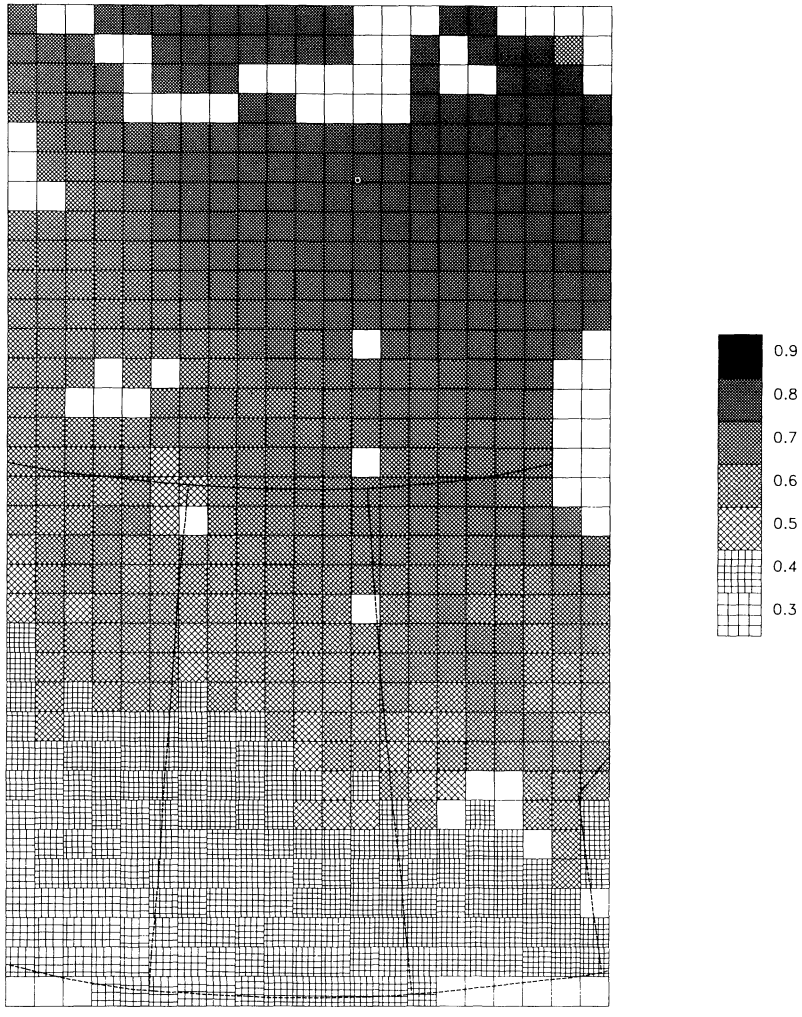

Figure 6. Unclassed choropleth map of Stefan frost number F_{s+}, constructed using nonuniform soil properties. Grid cells correspond to 34 × 21 lattice on which Figures 1–5 are based. Permafrost-free areas are represented by horizontal/vertical shading; areas underlain by permafrost are represented by diagonal shading. Divisions in legend provide representative shading densities at equal intervals over range of values on map. Unshaded cells represent locations of large water bodies or U.S. territory (bottom row).

extent of contemporary permafrost. Although an excellent impression of permafrost distribution may be obtained without a detailed description of input variables, interpretation of the causal factors behind the distribution may be impossible for map users without access to data used in constructing the map. Because a great deal of information can be contained in F_{s+} computed for multilayer soil systems and because of the ratio nature of the index, maps depicting the distribution of the frost number are not effective tools for interpreting the operation of the physical system. The frost number's primary usefulness lies in its ability to provide well-defined estimates of the areal extent of permafrost that are in close agreement with empirical delineations at small map scales. A series of maps in which soil properties are held constant within each map may be the most useful format for certain task-oriented purposes. With appropriate and carefully chosen symbolization, however, a single map constructed using spatially variable soil properties will yield the best overall impression of permafrost distribution.

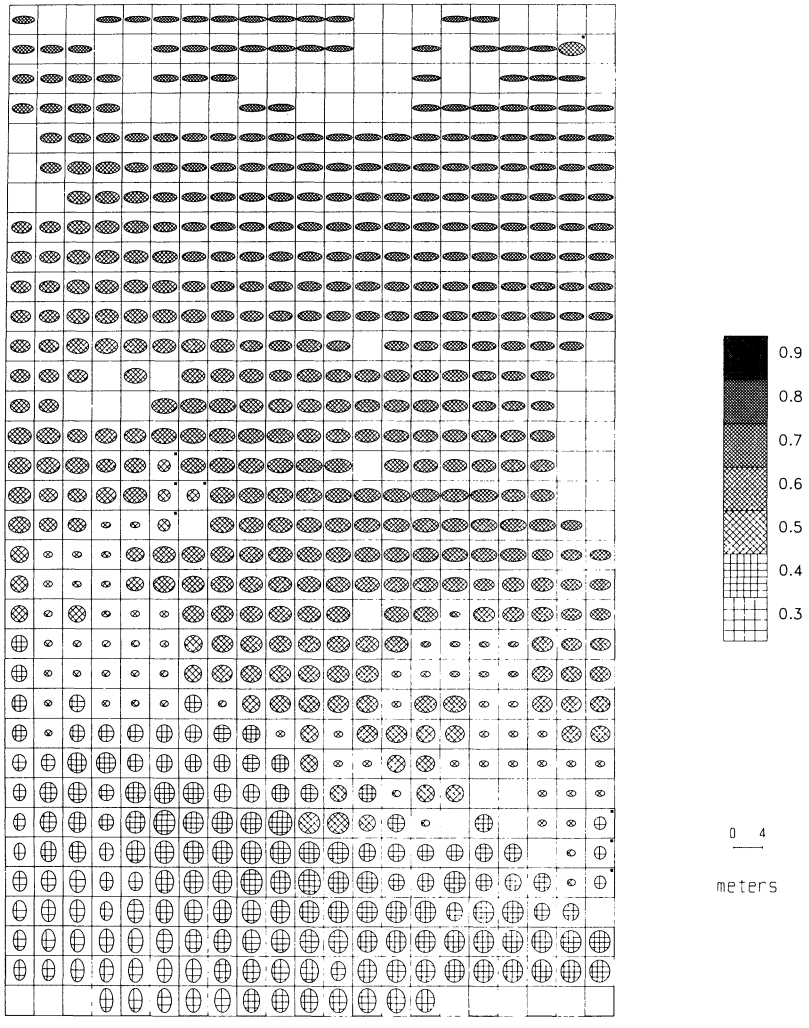

Figure 7. Ellipse map of Stefan frost number F_{s+}. Length of horizontal axis of ellipse is proportional to depth of freezing; length of vertical axis is proportional to depth of thawing. Cells with asterisk in upper right corner contain "Rockland Land Type"; lengths of ellipse axes in these cells should be multiplied by 10 to obtain depth to which perceptible temperature changes occur. Shading within ellipse is proportional to magnitude of F_{s+}. Orientation of shading indicates presence or absence of permafrost. Bar scale refers to depth of frost/thaw penetration.

Acknowledgments

Research leading to this paper was supported by the Division of Polar Programs, U.S. National Science Foundation, Grant #DPP–8117124. I am grateful to J. A. Heginbottom, K. M. Hinkel, S. I. Outcalt, M. G. Wilder and an anonymous reviewer for critical comments. Dr. Outcalt suggested the use of cubic splines and kindly allowed me to use his lattice-tuning program for the interpolations on which Figures 1–5 are based. Dr. W. A. Ericson (Director, Statistical Research Laboratory, University of Michigan) suggested the sampling strategy.

Notes

1. Ives (1979, 235) defined contemporary permafrost as "perennially frozen ground that is compatible with existing climatic and terrain conditions."
2. Results from a variant of Equation (3) (Nelson and Outcalt 1983, Equation 17) for "average" snow-cover thickness have been compared with actual snow-cover data for 199 Canadian stations, stratified by vegetation association. The equation accounted for 50–80 percent of the variance in three data subsets (Stuart 1985).
3. Treatment of the snowpack as a homogeneous

solid in which only conductive heat transfer occurs is an obvious oversimplification. Ideally, the effects of vapor transport, latent heat, and spatially and temporally variable snow density would be incorporated in a value of "apparent" thermal diffusivity in Equation (4). This problem is being pursued by A. Stuart (1985). The method used in this paper does provide a significant reduction of the freezing index at the ground surface, is consistent with the approximative nature of the overall methodology, and constitutes a considerable improvement over complete neglect of snow-cover effects. Treatment of the snow cover as a simple insulation layer in permafrost engineering problems is fairly common practice (e.g., Kudryavtsev 1977; Lachenbruch 1959). It is important to recognize that the definition of "average snow thickness" used in this paper is compatible only with small geographical scales. Redistribution of the snowpack by wind is an almost universal characteristic of regions in which snow accumulates (e.g., Thorn 1978). Equation (3) provides an estimate of snow thickness that is proportional to snowfall but makes no assumptions about redistribution of the snow by wind. Mapping the frost number at large geographical scales would require incorporation of topoclimatological effects, including snowdrift patterns.

References

Bilello, M. A. 1969. *Relationships between climate and regional variations in snow-cover density in North America*. U.S. Army Cold Regions Research and Engineering Laboratory, Research Report 267. Hanover, N.H.

Bostock, H. S. 1970. Physiographic subdivisions of Canada. In *Geology and economic minerals of Canada,* ed. R. J. W. Douglas, pp. 11–30. Geological Survey of Canada, Economic Geology Report no. 1, vol. 1. Ottawa.

Brown, R. J. E. 1967. *Permafrost in Canada*. Geological Survey of Canada Map 1246A and National Research Council of Canada, Division of Building Research Map NRC-9769. Scale 1:7,603,200. Ottawa.

———. 1974. Some aspects of airphoto interpretation of permafrost in Canada. Division of Building Research, National Research Council of Canada, Technical Paper 409, Ottawa.

———. 1978. Permafrost Map of Canada. In *Hydrological atlas of Canada,* Plate 32. Scale 1:10,000,000. Ottawa: Department of Fisheries and Environment.

Brown, R. J. E., and Péwé, T. L. 1973. Distribution of permafrost in North America and its relationship to the environment: A review. In *Permafrost—North American contribution to the Second International Conference,* pp. 71–100. Washington, D.C.: National Academy of Sciences.

Brown, W. G. 1964. Difficulties associated with predicting the depth of freeze or thaw. *Canadian Geotechnical Journal* 1:215–26.

Canada Atmospheric Environment Service. 1982a. *Canadian climate normals*. Vol. 2. *Temperature, 1951–1980*. Toronto.

———. 1982b. *Canadian climate normals*. Vol. 3. *Precipitation, 1951–1980*. Toronto.

———. 1982c. *Canadian climate normals*. Vol. 4. *Degree days, 1951–1980*. Toronto.

———. 1982d. *Canadian climate normals*. Vol. 5. *Wind, 1951–1980*. Toronto.

———. 1982e. *Principal climatological station network* (map). Scale 1:7,500,000. Toronto.

Canada Department of Energy, Mines and Resources. 1972. *Soils of Canada* (map). Scale 1:5,000,000. Ottawa.

———. 1975. *Soil climates of Canada: Soil moisture* (map). Scale 1:10,000,000. Ottawa.

Clark, P. J., and Evans, F. C. 1954. Distance to nearest neighbor as a measure of spatial relationships in populations. *Ecology* 35:445–53.

Clayton, J. S.; Ehrlich, W. A.; Cann, D. B.; Day, J. H.; and Marshall, I. B. 1977. *Soils of Canada,* vol. 1, *Soil report*. Ottawa: Canada Department of Agriculture.

Cliff, A. D., and Ord, J. K. 1981. *Spatial processes: Models and applications*. New York: Methuen.

Conrad, V. 1946. Usual formulas of continentality and their limits of validity. *Transactions of the American Geophysical Union* 27:663–64.

Davis, J. C. 1973. *Statistics and data analysis in geology*. New York: Wiley.

French, H. M., and Gilbert, R. 1982. Periglacial phenomena near Churchill, Manitoba. *Naturaliste Canadien* 109:433–44.

Geological Survey of Canada. 1970. *Geological map of Canada*. Map 1250a. Scale 1:5,000,000. Ottawa.

Granberg, H. B. 1973. Indirect mapping of the snow-cover for permafrost prediction at Schefferville, Quebec. In *Permafrost—North American contribution to the Second International Conference,* pp. 113–20. Washington, D.C.: National Academy of Sciences.

Hare, F. K., and Thomas, M. K. 1979. *Climate Canada*. Toronto: Wiley.

Harlan, R. L., and Nixon, J. F. 1978. Ground thermal regime. In *Geotechnical engineering for cold regions,* ed. O. B. Andersland and D. M. Anderson, pp. 103–63. New York: McGraw-Hill.

Harris, S. A. 1981. Climatic relationships of permafrost zones in areas of low winter snow-cover. *Arctic* 34:64–70.

Heginbottom, J. A. 1984. The mapping of permafrost. *Canadian Geographer* 28:78–83.

Ives, J. D. 1974. Permafrost. In *Arctic and alpine environments,* ed. J. D. Ives and R. G. Barry, pp. 159–94. London: Methuen.

———. 1979. A proposed history of permafrost development in Labrador-Ungava. *Géographie Physique et Quaternaire* 33:233–44.

Johnston, G. H.; Ladanyi, B.; Morgenstern, N. R.; and Penner, E. 1981. Engineering characteristics of frozen and thawing soils. In *Permafrost: Engineering design and construction,* ed. G. H. Johnston, pp. 73–147. Toronto: Wiley.

Jumikis, A. R. 1977. *Thermal geotechnics*. New Brunswick, N.J.: Rutgers University Press.

Kersten, M. S. 1949. Thermal properties of soils. *Uni-*

versity of Minnesota Engineering Experiment Station Bulletin 28:1–227.

King, J. T. 1984. *Introduction to numerical computation.* New York: McGraw-Hill.

Kudryavtsev, V. A. 1977. Fundamentals of frost forecasting in geological engineering investigations. U.S. Army Cold Regions Research and Engineering Laboratory, Draft Translation 606, Hanover, N.H.

Lachenbruch, A. H. 1959. Periodic heat flow in a stratified medium with application to permafrost problems. *U.S. Geological Survey Bulletin* 1083-A: 1–36.

———. 1968. Permafrost. In *The encyclopedia of geomorphology,* ed. R. W. Fairbridge, pp. 833–38. New York: Reinhold.

Langham, E. J. 1981. Physics and properties of snowcover. In *Handbook of snow. Principles, processes, management and use,* ed. D. M. Gray and D. H. Male, pp. 275–337. Toronto: Pergamon.

Lunardini, V. J. 1981. *Heat transfer in cold climates.* New York: Van Nostrand Reinhold.

MacFarlane, D. K. 1969. Special construction problems. In *Muskeg engineering handbook,* ed. D. K. MacFarlane, pp. 209–60. Toronto: University of Toronto Press.

Muller, S. W. 1945. *Permafrost or permanently frozen ground and related engineering problems.* Ann Arbor, Mich.: J. W. Edwards.

Nelson, F., and Outcalt, S. I. 1983. A frost index number for spatial prediction of ground-frost zones. In *Permafrost: Proceedings of the Fourth International Conference,* vol. I, pp. 907–11. Washington, D.C.: National Academy Press.

Panofsky, H. A., and Brier, G. W. 1968. *Some applications of statistics to meteorology.* University Park: Pennsylvania State University Press.

Paré, D. 1984. The occurrence of permafrost in peatlands. *Geoscope* 14:1–18.

Paterson, W. S. B. 1981. *The physics of glaciers.* New York: Pergamon.

Péwé, T. L. 1975. *Quaternary geology of Alaska.* U.S. Geological Survey Professional Paper 835. Washington, D.C.

Pihlainen, J. A. 1962. An approximation of probable permafrost occurrence. *Arctic* 15:151–54.

Rhynsburger, D. 1973. Analytic delineation of Thiessen polygons. *Geographical Analysis* 5:133–44.

Stuart, A. 1985. Personal communication, Kel-Research Corporation, 850-A, Alness Street, Suite 9, Downsview, Ontario, M3J 2H5.

Sumgin, M. I. 1940. *General permafrostology* (in Russian). U.S.S.R. Academy of Sciences.

Tarnocai, C. 1972. Some characteristics of cryic organic soils in northern Manitoba. *Canadian Journal of Soil Science* 52:485–96.

Terzaghi, K. 1952. Permafrost. *Journal of the Boston Society of Civil Engineers* 39:1–50.

Thorn, C. E. 1978. The geomorphic role of snow. *Annals of the Association of American Geographers* 68:414–25.

Tobler, W. R. 1973. Choropleth maps without class intervals? *Geographical Analysis* 5:262–65.

———. 1979. Lattice tuning. *Geographical Analysis* 11:36–44.

Zoltai, S. C. 1971. Southern limit of permafrost features in peat landforms, Manitoba and Saskatchewan. *Geological Association of Canada Special Paper* 9:305–10.